Psychophysiology, 52 (2015), 1441–1450. Wiley Periodicals, Inc. Printed in the USA.

DOI: 10.1111/psyp.12508

Heartbeat-related EEG amplitude and phase modulations from wakefulness to deep sleep: Interactions with sleep spindles and slow oscillations

JULIA LECHINGER,[a,b,c] DOMINIK PHILIP JOHANNES HEIB,[a,b,c] WALTER GRUBER,[a,c] MANUEL SCHABUS,[a,b,c] AND WOLFGANG KLIMESCH[a,c]

[a]Department of Psychology, Division of Physiological Psychology, University of Salzburg, Salzburg, Austria
[b]Laboratory for Sleep and Consciousness Research, University of Salzburg, Salzburg, Austria
[c]Centre for Cognitive Neuroscience (CCNS), University of Salzburg, Salzburg, Austria

Abstract

Based on physiological models of neurovisceral integration, different studies have shown how cognitive processes modulate heart rate and how the heartbeat, on the other hand, modulates brain activity. We tried to further determine interactions between cardiac and electrical brain activity by means of EEG. We investigated how the heartbeat modulates EEG in 23 healthy controls from wakefulness to deep sleep and showed that frontocentral heartbeat evoked EEG amplitude and phase locking (as measured by intertrial phase locking), at about 300-400 ms after the R peak, decreased with increasing sleep depth with a renewed increase during REM sleep, which underpins the assumption that the heartbeat evoked positivity constitutes an active frontocortical response to the heartbeat. Additionally, we found that individual heart rate was correlated with the frequency of the EEG's spectral peak (i.e., alpha peak frequency during wakefulness). This correlation was strongest during wakefulness and declined linearly with increasing sleep depth. Furthermore, we show that the QRS complex modulates spindle phase possibly related to the correspondence between the frequency of the QRS complex and the spindle frequency of about 12–15 Hz. Finally, during deep sleep stages, a loose temporal coupling between heartbeats and slow oscillation (0.8 Hz) could be observed. These findings indicate that cardiac activity such as heart rate or individual heartbeats can modulate or be modulated by ongoing oscillatory brain activity.

Descriptors: EEG oscillations, Heartbeat evoked potential, Heart rate, Sleep spindles, Slow oscillations

Some theoretical work and experimental research has taken a system's perspective on mental functions. Recently, Klimesch (2013) has even proposed a metric of the body's oscillatory architecture, which should not only fit brain oscillations (delta, theta, alpha, beta, and gamma), but should also include, for example, cardiac activity or, more specifically, heart rate, which would even serve the model as a scaling factor. The organization of oscillatory activity into one describable system provides a reasonable explanation for the emergence of functioning communication between different networks that are tuned to exactly those frequencies described by the model. Concerning oscillatory brain activity, the necessity for different networks to communicate in order to coherently process contents is obvious. From EEG and magnetoencephalography research, there is ample evidence for different types of between-frequency coupling (Jensen & Colgin, 2007; Lakatos et al., 2005; Palva, Palva, & Kaila, 2005). However, the potential necessity for a coupling between brain and body oscillations is less obvious. Within the organization of peripheral body activity, however, the relevance for a coupling of different oscillators has again been well documented. The heart, for example, can be seen as a permanent oscillator, which has been shown to be coupled to other bodily oscillators such as respiration (Censi, Calcagnini, & Cerutti, 2002; Cysarz et al., 2004; Novak et al., 1993; Saul, Kaplan, & Kitney, 1988).

Physiological research has revealed a coupling of encephalic and cardiac activity. In their model of neurovisceral integration, Thayer and Lane (2009), proceeding from the work of French physiologist Claude Bernard, suggest that areas in the frontal lobe influence heart rate (HR) and heart rate variability (HRV). They assume that prefrontal cortical areas, including the orbitofrontal cortex and the medial prefrontal cortex, inhibit the amygdala via GABAergic neurons. As the amygdala generally exerts an excitatory influence on HR, increased prefrontal activation eventually leads to a decrease in HR and increase in HRV. On the other hand, disinhibition of the amygdala is associated with increased HR and

We thank Martin Wolters for his help with data preparation and Christine Blume for her valuable comments on the manuscript. JL and DPJH are supported by the Doctoral College "Imaging the Mind" (FWF; W1233-G17).

Address correspondence to: Julia Lechinger, Department of Psychology, Division of Physiological Psychology, University of Salzburg, Hellbrunnerstraße 34, 5020 Salzburg, Austria. E-mail: julia.lechinger@sbg.ac.at

PSYCHOPHYSIOLOGY

decreased HRV. This inhibitory control of prefrontal areas via the central autonomic network has been proposed to render the organism more flexible and more adaptive to environmental changes (for a review, refer to Thayer & Lane, 2009). The influence of cognitive processes on HR is well documented by studies investigating heartbeat acceleration/deceleration (Fowles, Fisher, & Tranel, 1982; Mies, van der Veen, Tulen, Hengeveld, & van der Molen, 2011; Panitz, Wacker, Stemmler, & Mueller, 2013; van der Veen, van der Molen, Crone, & Jennings, 2004). As an example, Lawrence and Barry (2010) found that within a few seconds after hearing a 1000 Hz beep HR decelerated, but accelerated when subjects were asked to silently count the beeps.

An interesting kind of brain-heart communication is documented by EEG research on interoceptive awareness, focusing on the so-called heartbeat evoked potential (HEP; e.g., Pollatos & Schandry, 2004), which is most prominent over the somatosensory cortex and the (pre)frontal cortex. In general, the vagus nerve contains 80–85% afferent fibers, their destination being the solitary tract of the brainstem (Jänig, 1996). Projections from there reach to the parabrachial nuclei and the locus coeruleus, from which visceral information is, among others, passed on to the hypothalamus and the thalamus and finally to regions in the cortex, such as the somatosensory cortex, the cingulate gyrus, the frontal cortex, and the insular cortex. Pollatos and Schandry (2004) asked healthy participants to silently count their own heartbeat (without taking their pulse). They found that the average HEP activity between 250 and 350 ms after the R wave was significantly higher in the good as compared to the poor heartbeat perceivers, while electrocardiographic (ECG) mean scores did not differ in that time window. This result was well in line with earlier studies, which had already shown relationships between cardiac awareness and HEP amplitude (Montoya, Schandry, & Müller, 1993; Schandry & Weitkunat, 1990). Furthermore, HEP amplitudes have also been related to stress (Gray et al., 2007) and empathy (Fukushima, Terasawa, & Umeda, 2011). Recently, Park, Correia, Ducorps, and Tallon-Baudry (2014) also showed a fascinating relationship between cardiac activity and visual awareness, where the detection of faint visual stimuli was associated with the amplitude of the heartbeat evoked response. The authors argue that heartbeat evoked responses might provide information related to the subjective dimension of visual experience or, in other words, that visceral (Critchley & Harrison, 2013) together with proprioceptive (Blanke, 2012) information might promote a neural subjective frame required for conscious experience (Park & Tallon-Baudry, 2014).

In the present study, we investigated how the heartbeat and heart rate might influence ongoing oscillatory EEG activity. In order to also address the question of how different background activity modulates or is modulated by cardiac activity, we investigated EEG responses from wakefulness to deep sleep. While falling asleep, the EEG changes significantly. At first, during light sleep Stage 1 (S1), alpha power decreases, followed by the appearance of sleep spindles with a frequency of 12–15 Hz indicating the transition to S2. The sleep spindle is a thalamocortical mechanism originating from GABAergic reticular thalamic neurons, thalamocortical cells, and cortical pyramidal neurons, supposedly inhibiting the forwarding of visual and auditory input (Steriade, McCormick, & Sejnowski, 1993). It has been shown that the processing of auditory stimuli that appear during a spindle is largely restricted (Schabus et al., 2007). With increasing sleep depth, brain activity becomes more monotonous and is characterized by higher amplitude activity in a slower frequency range. In deep sleep, large amplitude slow oscillations (~0.8 Hz) become evident (Achermann & Borbely, 1997). They are supposed to reflect an alternating pattern of hyperpolarization (down-state) and depolarization (up-state) of thalamo/cortical networks (Csercsa et al., 2010; Steriade, Contreras, Curro Dossi, & Nunez, 1993) and have been found to travel over the cortex (Massimini, Huber, Ferrarelli, Hill, & Tononi, 2004). The slow oscillation has been shown to modulate sleep spindle activity and, thereby, to even group the occurrences of detectable spindle events (Mölle, Eschenko, Gais, Sara, & Born, 2009).

In summary, the aim of this study was to investigate cortical responses to the heartbeat from wakefulness to deep sleep. Although the HR and HRV change during sleep, the ECG dynamics of a single heartbeat (which are monitored in the present study) remain remarkably constant. First of all, we investigated the heartbeat evoked positivity at about 300–400 ms, and hypothesized that, if this frontocortical response relates to cardiac awareness, then its amplitude should decrease with sleep depth. Furthermore, the transition through different sleep stages represents changes in brain state, which are accompanied by changes in the oscillatory characteristics and present with specific rhythmic activation patterns such as sleep spindles (during non-rapid eye movement [NREM] sleep S2) or slow oscillations (during deep sleep). We were, therefore, interested in whether and how the heartbeat is related to (or even modulates) characteristic state-dependent brain activity and investigated potential relationships with sleep spindles and slow oscillations.

Method

Participants

EEG was analyzed in 23 subjects recorded in a former study on sleep and memory consolidation (Schabus et al., 2004). The complete sample consisted of 24 healthy subjects (12 females) aged between 20 and 30 years (mean age = 24.42 years, $SD = 2.59$). However, one participant was excluded due to corrupted ECG signal. All analyzed subjects were healthy sleepers as assessed by a polysomnographic screening night, questionnaires, and wrist actigraphy. For further details, see the original study. For the current study, only control nights (without prior memory tasks) were selected. Objective sleep data for the included 23 subjects were: total sleep time (min) = 433.80, $SD = 33.10$; sleep efficiency = 90.63, $SD = 5.46$; number of awakenings = 14.52, $SD = 9.43$; time in S1 (min) = 39.50, $SD = 15.30$; time in S2 (min) = 202.74, $SD = 35.19$; time in S3 (min) = 40.22, $SD = 14.47$; time in S4 (min) = 63.41, $SD = 21.71$; time in REM (min) = 87.93, $SD = 21.57$. The study was conducted in compliance with the code of ethics of the World Medical Association (Declaration of Helsinki).

EEG Recording

The EEG was recorded during a night of sleep using SynAmps EEG amplifiers (NeuroScan Inc., El Paso, TX). As wakefulness, the period prior to sleep onset was used in order to have comparable environmental conditions between wake and sleep. Twenty-two gold-plated silver electrodes (Fp1, FPz, Fp2, FCz, F7, F3, Fz, F4, F8, T3, C3, Cz, C4, T4, T5, P3, Pz, P4, T6, O1, Oz, O2 as well as A1 and A2 for later rereferencing) were placed according to the International 10-20 system. Furthermore, electrooculography, ECG, electromyography, and respiration were recorded. All signals were online referenced to FCz, digitized with 250 Hz sampling

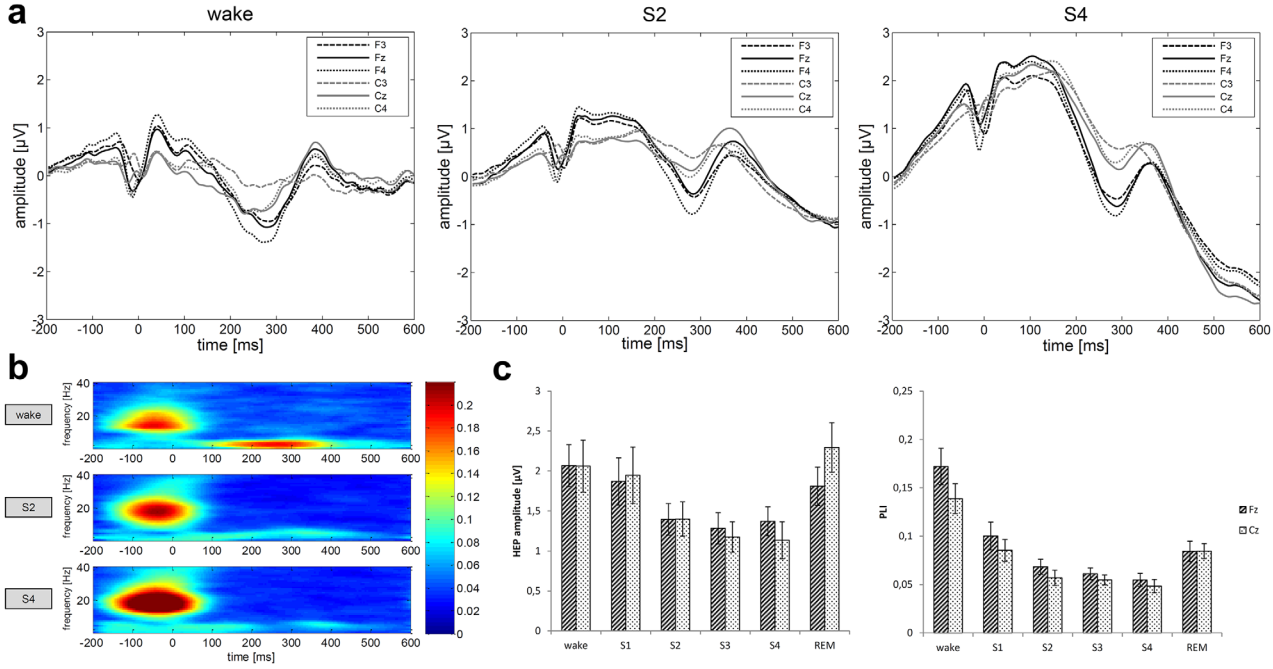

Figure 1. EEG response time locked to the heartbeat from wake to sleep. a: ERPs time locked to the heartbeat on frontal and central positions F3, Fz, F4, C3, Cz, C4. Only responses during wake, S2, and S4 are depicted. Time point zero corresponds to the R peak as detected in the ECG. b: The 2–6 Hz phase-locking index (PLI) corresponding to the heartbeat evoked positivity again decreases from wakefulness to deep sleep. Time point zero corresponds to the R peak. c: Average heartbeat evoked peak-to-peak amplitude and PLI (averaged from 280–400 ms) from wake to deep and REM sleep corresponding to (a) and (b). Note the systematic decrease in amplitude and phase locking from wake to deep sleep accompanied by a renewed increase during REM sleep.

rate, and filtered in a broad frequency band (0.10 Hz high-pass filter; 70 Hz low-pass filter; 50 Hz notch filter).

EEG Analysis

For heartbeat evoked potentials and heartbeat evoked phase response analyses, all signals were first rereferenced against both mastoids (average A1–A2), IIR-filtered between 0.3 and 40 Hz using BrainVision Analyzer 2.02 (BVA, Brain Products Inc., Gilching, Germany). Major artifacts were discarded manually. R peaks were automatically detected in the ECG channel with a BVA built-in algorithm and afterwards visually inspected. Epochs containing wrongly detected R peaks were manually corrected or discarded from further analysis. The number of R peaks that went into final analysis was restricted to 1,000 per sleep stage, per subject. This restriction was applied to lessen the gap in the number of R peaks between the single sleep stages, because a lot more time was spent in S2 than in the other stages, while the least time was spent in wake.

Sleep was scored automatically (Somnolyzer 24*7; The Siesta Group, Anderer et al., 2005; Schimicek, Zeitlhofer, Anderer, & Saletu, 1994) and manually verified by a sleep scoring expert according to Rechtschaffen and Kales (1968) criteria.

To determine the spectral peak frequency of each subject during the different wake/sleep stages, the signal during each sleep stage was segmented into 6-s segments (in order to get a sufficient frequency resolution), fast Fourier transformed, and averaged over segments. The frequency of the spectral peak was determined over occipital electrode Oz.

Evoked potentials (EP) were calculated by segmenting the signal relative to the R peak from −200 to +600 ms, and averaging all single trials per sleep stage per subject. To test the effect of the sleep spindle on EP amplitudes, only R peaks appearing within S2 sleep spindles were averaged. Since slow wave activity became larger in amplitude with increasing sleep depth that was still evident in the average response time locked to the R peak, we calculated peak-to-peak amplitude (the negative peak amplitude preceding the positive peak was subtracted from the positive peak amplitude) instead of absolute amplitude in order to get a realistic idea of the amplitude changes in the heartbeat-related positivity. Negative peaks were automatically detected in a time window from 200–320 ms, positive peaks were detected within 320–450 ms after R peak. Those time windows were chosen based on visual inspection of the group average ERP.

Phase-locking analyses (phase-locking index, PLI) according to Lachaux and colleagues (Lachaux, Rodriguez, Martinerie, & Varela, 1999) were conducted with the same segments. The PLI is calculated on phase only mostly independent from amplitude modulations. Phase was received through Hilbert transformation. The PLI represents the amount of phase locking between trials within one electrode. For statistical PLI analysis, the PLI in the frequency band with the strongest reactivity in the time window of the evoked positivity (2–6 Hz) was averaged from 280–400 ms. This time window was chosen because it showed the best overlap in peak activity over all sleep stages including REM. In the waking state, however, an increased phase locking could already be detected a bit earlier (see Figure 1b).

Spindle Detection

Automatic spindle detection was performed on electrode position C4 based on a further development (Anderer et al., 2005) of the

band-pass filtering method described by Schmicek et al. (1994). The EEG signal was filtered with a phase-linear Butterworth band-pass filter in the frequency range of 10–18 Hz, and the instantaneous amplitude of this filtered signal was determined by Hilbert transformation. Thereafter, the automatic sleep spindle detection was performed. In a first step, the algorithm identified all "possible" spindle episodes with the band-pass filtering method described by Schmicek et al. (1994) using the following detection criteria: (a) spindle duration between 0.3–2 s, (b) a frequency range of 11–15 Hz, and (c) a minimal amplitude of 12 μV. In a next step, "real" spindle episodes were determined by means of a linear discriminant analysis using five log-transformed spindle features (duration and mean amplitudes in the frequency bands: spindle, theta, alpha, and fast beta) of the possible spindles.

Slow Oscillation Detection

Slow oscillations were detected over electrode Fz during S3 and S4 sleep. First, all signals were low-pass filtered at 30 Hz, rereferenced to the average of A1 and A2, low-pass filtered at 4 Hz, and down-sampled to 100 Hz. Subsequently, to detect slow oscillations, standard detection criteria were applied using own-built MATLAB routines (MathWorks, Natick, MA: (a) a positive zero crossing follows a negative zero crossing in a time window of 0.3–1 s, (b) a peak negativity between such two zero crossings falls below -80 μV, and (c) an amplitude difference between the peak negativity and a subsequent positive peak of at least 140 μV (Massimini et al., 2004).

To check for a possible grouping of the heartbeat with the slow oscillation, we segmented slow oscillations from -800 to $+800$ ms relative to their middle zero crossing (i.e., that all segments had the same length independent of the actual slow oscillation duration) and determined the individual absolute time difference between R peaks appearing within this time window and the zero crossing. We refrained from a grouping to the relative length of either the negative or the positive wave (e.g., split both lengths into the same amount of time bins) as well as from a grouping with respect to the phase, because the positive wave was about 1.5 to 2 times the length of the negative wave, which increases the general probability for an event to appear in the (longer) positive wave.

Statistical Analysis

EP amplitude and PLI were subjected to analyses of variance (ANOVAs) for repeated measures.

For the changes with increasing sleep depth, ANOVAs Sleep Stage (wake vs. S1 vs. S2 vs. S3 vs. S4 vs. REM) $\times$ Laterality (F7 vs. F3 vs. Fz vs. F4 vs. F8 and C3 vs. Cz vs. C4) as well as Sleep Stage $\times$ Topography (Fz vs. Cz) were calculated for both dependent variables. Post hoc comparisons were done using T tests for dependent variables (corrected for multiple comparisons according to Benjamini & Hochberg, 2000). Whenever sphericity could not be assumed, the ε value according to the Huynh-Feldt correction will be mentioned.

To investigate a general relationship between the heart rate and EEG activity, we correlated heart rate (Hz) with the spectral peak frequency during the different wake/sleep stages using Pearson correlations.

Furthermore, EPs and PLI were compared between general S2 and S2 during spindle events using dependent T tests. Differences in PLI (spindle frequency 11–15 Hz) relative to the R peak occurring during an S2 spindle versus PLI relative to R peaks occurring in general S2 (irrespective of spindle presence) vs. PLI relative to S2 spindle onset without co-occurring R peaks were tested using ANOVAs Topography (Fz vs. Cz) $\times$ Condition (R peaks during spindles vs. R peaks during general S2 vs. spindles without R peaks). For this analysis, the PLI in the 11–15 Hz range was averaged for a period of 600 ms (segments with heartbeats: -200–400 ms with respect to the R peak [for heartbeat and spindle segments, the spindle onset had to be in a time window between -200–0 ms with respect to the R peak]; segments with spindle but without heartbeat: 0–600 ms with respect to spindle onset).

Slow oscillation grouping was statistically tested comparing the number of heartbeats during the slow oscillation down- (-750–0 ms relative to the zero crossing) and up-state (0–750 ms relative to the zero crossing) using a nonparametric Wilcoxon rank sum test.

Results

Heartbeat Evoked Positivity

Visual inspection of the evoked potentials indicated that, while the EEG response directly corresponding to the R peak (i.e., "R peak artifact") was highest at occipital sites with decreasing and even changing polarity at frontal sites, a heartbeat evoked positivity at about 300–450 ms after the R peak was highest at frontal sites, disappearing at parieto-occipital sites (cf. Figure 1). Furthermore, the amplitude of the R peak artifact did not visibly change over sleep stages, whereas the amplitude of the heartbeat evoked positivity decreased from wake to deep sleep, with a renewed increase during REM sleep. Interestingly, heartbeats appearing simultaneously with a sleep spindle did not produce a clearly discernible heartbeat evoked positivity. The ERP analysis confirmed these observations. ANOVA Sleep Stage (wake vs. S1 vs. S2 vs. S3 vs. S4 vs. REM) $\times$ Laterality (F7 vs. F3 vs. Fz vs. F4 vs. F6) for the frontal topography showed main effects for both factors (sleep stage: $F(5,110) = 3.74$, $p < .01$, $\varepsilon = .76$; laterality: $F(4,88) = 23.59$, $p < .001$, $\varepsilon = .47$), with general peak-to-peak amplitudes decreasing from right (F8) to left (F7) as well as a continuous decrease from wake to deep sleep.

Amplitudes during REM were again comparable to S1 sleep. Multiple T tests showed that on electrodes Fz and F4 all sleep stages except S1 and REM presented with decreased amplitudes as compared to wake, while electrode F3 exhibited a decrease in amplitude only in S2 and S3, $ts(22) > 2.26$, $p < .05$, one-tailed, corrected for multiple comparisons. Furthermore, all frontal electrodes showed decreased EP amplitudes during S2 spindles as compared to general S2, $ts(22) > 2.14$, $p < .05$, one-tailed, corrected for multiple comparisons.

For the central topography, again both factors presented with a main effect (sleep stage: $F(5,110) = 8.18$, $p < .001$, $\varepsilon = .72$; laterality (C3 vs. Cz vs. C4): $F(2,44) = 22.18$, $p < .001$). T tests again showed that on electrodes Cz and C4 all sleep stages except S1 and REM presented with decreased amplitudes as compared to wake and on C3 also at least S2 and S4 showed significantly lower amplitudes, $ts(22) > 2.45$, $p < .05$, one-tailed, corrected for multiple comparisons. ANOVA Sleep Stage $\times$ Topography (Fz vs. Cz) only confirmed the main effect for sleep stage but did not confirm the observable decrease from the frontal to the central topography (sleep stage: $F(5,110) = 7.77$, $p < .001$, $\varepsilon = .70$, topography: $F(1,22) = 0.9$, $p = n.s.$)

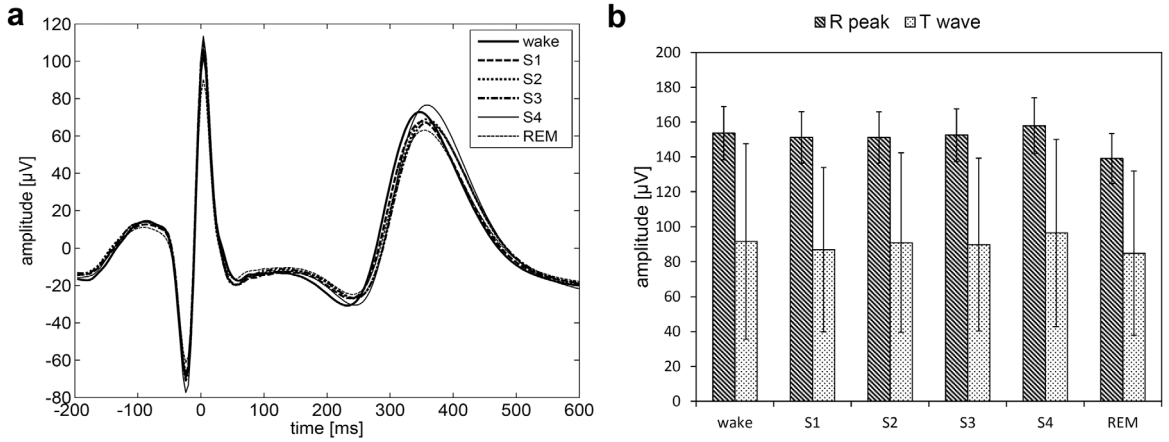

Figure 2. Average ECG components from wake to deep sleep. a: Average heartbeats (Q, R, S, T components) as measured by the ECG from wake to sleep. b: R peak and T wave amplitudes from wake to sleep. The mere amplitudes did not significantly change over sleep stages.

Heartbeat Evoked Phase Locking (PLI)

The heartbeat evoked positivity was accompanied by an increase in PLI from 2–6 Hz, which decreased in the same manner from wake to deep sleep, including a renewed increase during REM sleep (ANOVA Sleep Stage [wake vs. S1 vs. S2. vs. S3 vs. S4 vs. REM] × Topography [Fz vs. Cz]: sleep stage: $F(5,10) = 25.72$, $p < .001$, $\varepsilon = .49$). *T* tests revealed that all stages showed a decreased PLI as compared to wake, $ts(22) > 4.22$, $p < .001$, one-tailed, corrected for multiple comparisons. Furthermore, delta PLI was higher frontally than centrally (topography: $F(1,22) = 6.79$, $p < .05$) for wake, S1, and S2, $ts(22) > 1.99$, $p < .05$, one-tailed, corrected for multiple comparisons.

Control Analysis for Evoked Potentials and EEG Frequency Response to the QRS Complex

To test for possible difference in the heartbeat evoked potential as measured by the ECG, we tested whether the ECG R and T peak amplitudes changed over sleep stages. Only a marginally significant decrease in R peak amplitude could be observed for REM as compared to wake, $t(22) = 2.00$, $p = .06$, uncorrected. All other comparisons did not result in any significant R peak, $ts(22) < 0.82$, $p = n.s.$ (cf. Figure 2) or T wave differences, $ts(22) < 1.61$, $p = n.s.$ (cf. Figure 2).

On scalp level, the R peak was accompanied by an increased phase locking in the beta range (cf. Figure 1b). The frequency that showed the strongest phase locking changed from about 16.5 Hz (Cz) in waking to about 18.5 Hz in deep NREM sleep (ANOVA sleep stage with frequency [Hz] as dependent variable: $F(5,110) = 5.62$, $p < .001$). In a similar pattern, the spectral peak of the occipital EEG changed from 10.15 Hz to 13.60–13.72 Hz. Interestingly, the numeric relation between the spectral peak and peak PLI frequency was not simply 1:1 and did not even stay constant from wake to sleep.

Correlations Between Heart Rate and EEG Spectral Peak Frequency

During wakefulness, the average spectral peak frequency was 10.15 Hz and the average HR was 1.18 Hz. During NREM sleep S2–S4, the average spectral peak frequency was between 13.60–13.72 and the average HR was between 0.94–0.99 Hz. We found correlations between the individual heart rate and the EEG spectral peak frequency. The correlation was highest during wakefulness ($r = .48$, $p < .05$) and decreased with increasing sleep depth (S2: $r = .40$, $p = .056$; S3: $r = .34$, $p = n.s.$; S4: $r = .26$, $p = n.s.$, cf. Figure 3). Note that most subjects showed no spectral peak during S1 and REM and, therefore, no correlations were calculated. Furthermore, for the state-wake correlation, one subject had to be excluded due to a missing alpha peak.

Spindle Phase Modulation

Heartbeats occurring during S2 spindles produced a clearly visible ringing in the spindle frequency range (cf. Figure 4), which was not evident when spindles without co-occurring heartbeats were averaged with respect to their onset. Note that also heartbeats during general S2 (irrespective of spindle presence) did not produce a phase locking in the spindle frequency range. Statistical 11–15 Hz PLI analysis ANOVA Topography (Fz vs. Cz) × Condition (spindle without heartbeat vs. spindle with heartbeat vs. heartbeat without spindle) confirmed the main effect for condition, $F(2,44) = 29.11$, $p < .001$, $\varepsilon = .70$. *T* tests showed that on both topographies heartbeats occurring during a spindle produced a higher PLI in the spindle frequency range as compared to both spindles without heartbeats as well as heartbeats in general S2, $ts(22) > 3.64$, $p < .01$, corrected for multiple comparisons (cf. Figure 4b).

The same analysis was repeated for delta PLI. Here, both main effects (topography: $F(1,22) = 12.54$, $p < .01$; condition: $F(2,44) = 4.85$, $p < .05$, $\varepsilon = .74$) as well as the interaction Topography × Condition, $F(2,44) = 11.91$, $p < .001$, $\varepsilon = .72$, were significant. *T* tests showed that, on both sites Fz and Cz, delta (0.5–3.5 Hz) PLI was higher for heartbeats occurring with a spindle as compared to heartbeats occurring in general S2. In all cases, delta PLI was higher at Fz than on Cz. Still, on Cz delta phase locking was higher for spindles without heartbeats as compared to heartbeats in general S2, $ts(22) > 2.56$, $p < .05$, corrected for multiple comparisons.

Slow Oscillation Grouping

To further investigate synchronization processes between encephalic and cardiac activity, we additionally tested whether the slow oscillation as a mechanism known to induce or at least reflect a widespread pattern of cortical and subcortical hyper- and depolarization might show some connection with the timing of the

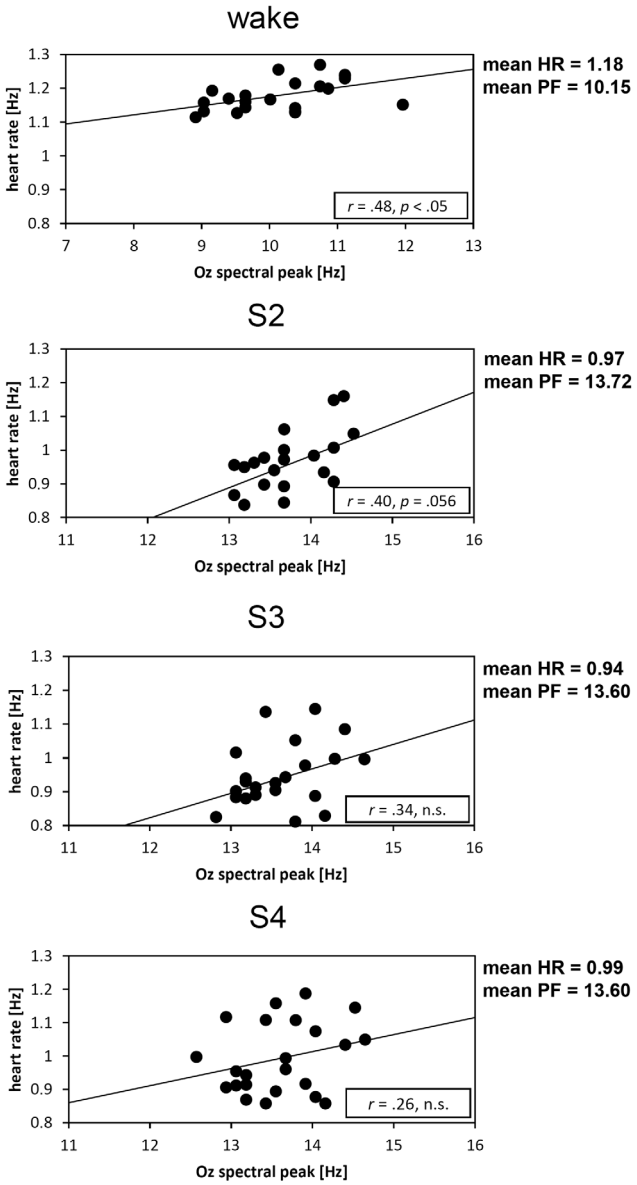

Figure 3. Correlations between EEG spectral peak frequency and heart rate. Significant and marginally significant correlations could only be found during wakefulness and intermediate NREM sleep S2. Correlation coefficients decreased linearly with increasing sleep depth. HR = heart rate; PF = peak frequency.

heartbeats. And indeed, we detected an increase of R peak appearances at the beginning of the positive peak (beginning depolarization phase) of the slow oscillation (cf. Figure 5). When comparing the number of R peaks during the negative wave (−750–0 ms) to the number during the positive wave (0–750 ms) over single subjects, a Wilcoxon rank sum test confirmed this observation ($Z = -3.19$, $p < .001$)

Discussion

We could show that the heartbeat evoked positivity at about 300–450 ms after the R peak declines with decreasing levels of consciousness. Interestingly, evoked amplitudes during REM sleep were quite similar to those in wakefulness, which might relate to the fact that, during REM cortical activity as represented by the EEG composition, is quite similar to wakefulness. In a study using transcranial magnetic stimulation (TMS) to test cortical excitability, Massimini and colleagues have shown that also TMS evoked responses during REM much more resemble the responses during wakefulness than those during NREM sleep (Massimini et al., 2010).

Furthermore, our results demonstrated that the sleep spindle as a thalamocortical inhibitory mechanism (preventing external visual and auditory input to be forwarded to the cortex) might also impair the cortical response to the heartbeat during NREM sleep S2. As mentioned earlier, information from the vagus nerve eventually reaches cortical areas also via the thalamus (Jänig, 1996). It can, therefore, be assumed that the spindle also inhibits the emergence of the heartbeat evoked positivity. One has to keep in mind, though, that the latter result could not be confirmed by the delta PLI analysis due to the increased background delta phase locking associated with the sleep spindle. In general, the amplitude of the heartbeat evoked component decreased from right to left, which was in line with previous studies and probably results from the fact that the heart is not symmetrically oriented in the body with the apex of the left ventricle pointing to the lower left side. Based on the fact that afferent fibers from the thorax mostly project to the contralateral side, this should result in stronger activation in the right as compared to the left hemisphere (Pollatos & Schandry, 2004).

Additionally, a significant correlation between the occipital spectral peak of the EEG and the HR during wakefulness provides evidence for a coupling between cardiac and electrical brain activity. The frequency relationship between those parameters is around 1:8 (i.e., about 1.2–10 Hz). This can be considered as an example that can be predicted from the algorithm suggested by Klimesch (2013) where the HR serves as a basic scaling factor for EEG frequencies.

Another key finding—as depicted in Figure 4—is that if a heartbeat coincides with a spindle event, the spindle becomes phase locked to the R peak. This conclusion can be derived from a comparison of spindle events occurring together with or without a heartbeat. Without a heartbeat, the calculation of the PLI is done with respect to the spindle onset. In this case, there is no phase locking of spindle oscillations relative to their onset. This is due to a weak (or lack of) time locking of the physiological spindle onset or the onset of the detection algorithm relative to spindle phase. In any case, this finding demonstrates that averaging spindle events does not exhibit a phase locking between spindles. This is not very surprising because a random jitter between spindles in the range of only about 30 ms (which is in the magnitude of a half period of a spindle oscillation) would completely abolish the appearance of phase locking and "spindle ringing." But if the PLI is calculated with respect to the R peak, spindles exhibit a significant increase in phase locking, which results in a spindle ringing in the ERP. The QRS complex itself has a frequency that lies in the spindle frequency range, but only lasts about 100 ms centered around the R peak. The spindle ringing, however, lasted up to about 350 ms after the R peak and was not present when R peaks in general S2 (irrespective of a present spindle event) were averaged. This finding clearly indicates that spindle phase is time locked to the R peak or, in other words, that the heartbeat operates to align or reset spindle phase, perhaps promoted by the fact that the frequency of the QRS complex matched the frequency range of the ongoing oscillatory activity.

And lastly, a temporal grouping of the heartbeat with the slow oscillation was evident in our data with the probability of R peak occurrences being highest at the positive slope of the slow oscillation upstate. The slow oscillation is supposed to reflect a bi-stable,

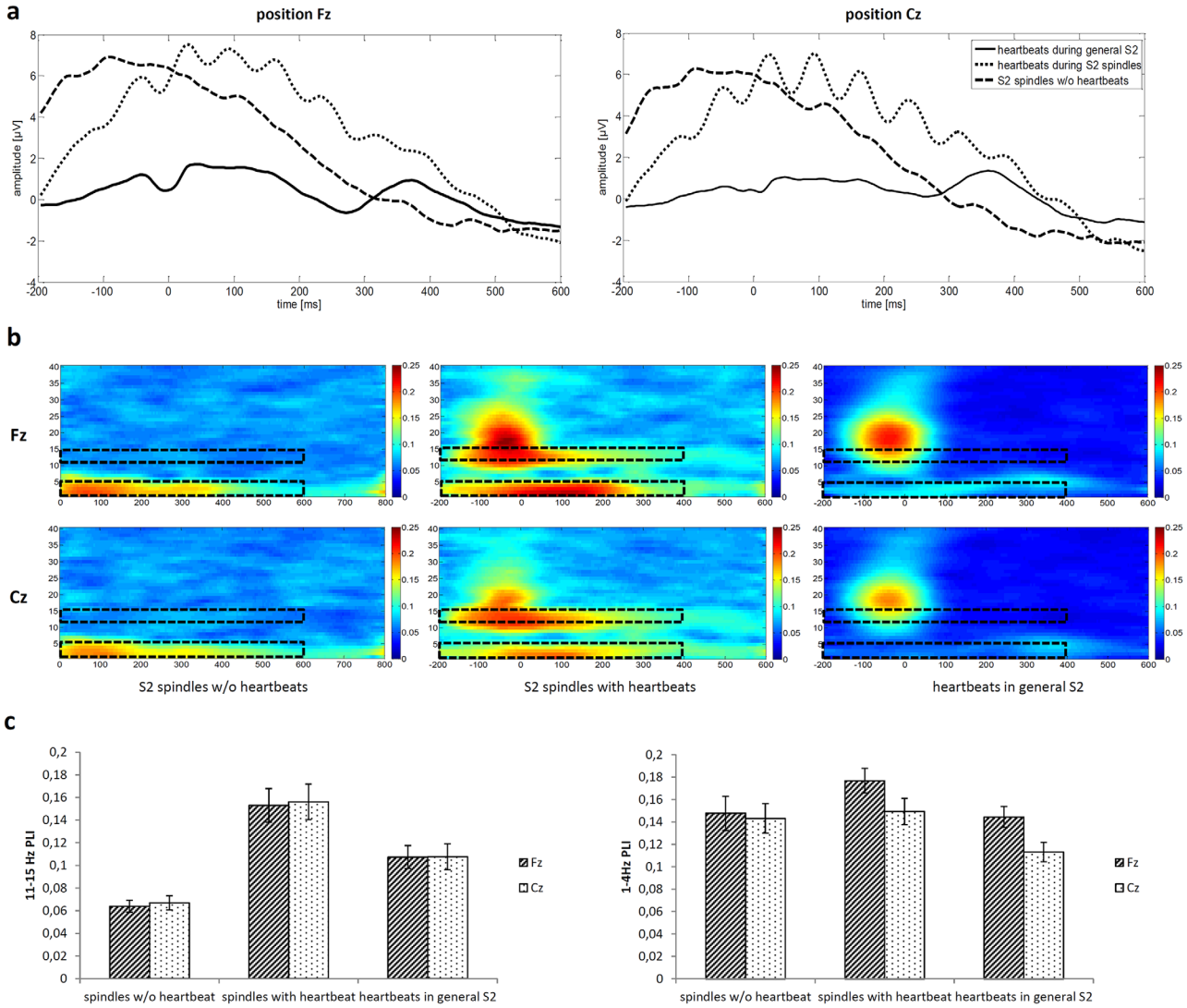

Figure 4. Modulation of spindle phase by co-occurring heartbeats. a: Fz and Cz ERPs in response to heartbeats occurring during general S2 sleep, heartbeat occurring during an S2 spindle, and averaged spindles without any heartbeat present. Time point zero corresponds to the R peak in heartbeat evoked responses, and to +200 ms after spindle onset in the spindle average. Note that heartbeats occurring during a spindle induce a visible phase locking (seen as ringing in the ERP). b: Corresponding PLI. Phase locking in the spindle frequency was highest for heartbeats occurring with an S2 spindle as compared to both spindles without co-occurring heartbeat as well as heartbeats in general S2. Upper row: Electrode Fz. Lower row: Cz. c: PLI averages in the 11–15 Hz (left) and the 1–4 Hz range (right), which were subjected to statistical analysis.

mostly frontoparietal pattern of hyperpolarization (negative wave) and depolarization (positive wave) of large neuronal assemblies. It has been shown that the depolarizing phase results in bursts of spindle activity (Mölle, Marshall, Gais, & Born, 2002), thereby slow oscillations group the occurrence of sleep spindles. Also, frontal populations engaged in heart rate modulation during wakefulness might undergo this pattern of hyper- and depolarization while exerting residual influence on heart rate regulation during deep sleep. This could explain the relationship between slow oscillation phase and R peak timing. In principle, the direction of influence could also be reversed, where the heartbeat could serve as a kind of pacemaker for slow oscillations. Although during sleep brain activity is largely internally organized, it can still be modulated by external input, as demonstrated by phenomena such as evoked K complexes (for a review, see Bastien, Crowley, & Colrain, 2002). Massimini and colleagues have also demonstrated the possibility of influencing ongoing oscillatory activity in the sleeping brain by TMS (Massimini, Boly, Casali, Rosanova, & Tononi, 2009; Massimini et al., 2007) showing that response to TMS largely differed in spatial and temporal architecture depending on consciousness state as well as TMS strength. Interestingly, they have found that during deep sleep, where much of the cortex shows a bi-stable activation pattern, TMS impulses < 1 Hz are able to evoke high amplitude slow oscillations that spread over the cortex (Massimini et al., 2007). The heartbeat perhaps also constitutes sufficiently strong input to the cortex to influence this bi-stability.

Concerning our results on heartbeat evoked responses from wake to sleep, one has to keep in mind that the study of heartbeat evoked potentials is complicated by artifacts. Mostly the QRS complex (ventricular systole) produces electrical artifacts in the shape of poorly formed QRS complexes in the EEG signal. The P (atrial systole) and T wave (ventricular relaxation) usually do not produce visible artifacts. Dirlich and colleagues (Dirlich, Vogl, Plaschke, & Strian, 1997) have studied cardiac field artifacts and found that the

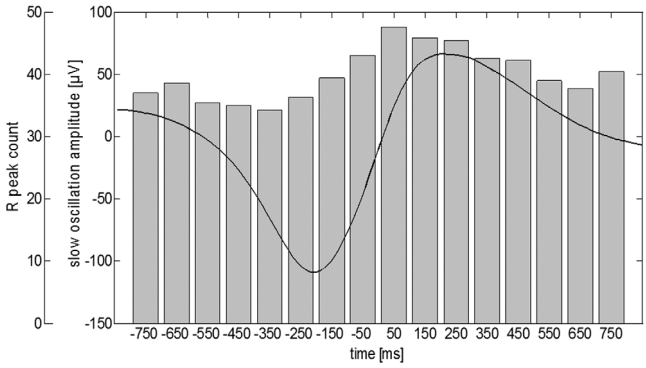

Figure 5. Average number of R peak appearances relative to the middle zero crossing of the slow oscillation. Time point zero corresponds to the slow oscillation's middle zero crossing. R peaks were counted in 100 ms time bins before and after 0. Bars depict the average number of R peaks detected during these 100 ms time bins over all subjects. Note the increase in the number of R peaks at the positive slope of the slow oscillation.

shorter the temporal distance from the R peak, the more variance in the EEG can be explained by ECG. We tried to control for cardiac field influence on the sleep stage-dependent evoked potential results by additionally subjecting the ECG R and T wave peak amplitude to the same ANOVAs as the late EEG component. These analyses did not indicate a potential "artificial" cause for the sleep-related decrease in heartbeat evoked EEG amplitude. Interestingly, however, the frequency of the PLI maximum, which corresponded to the QRS complex, actually increased from wake to deep sleep, although the shape of the QRS complex did not change. Another source of cardiac EEG artifact is the mechanical one arising from the pulse wave (arterial pressure wave). Visible pulse wave artifacts in the EEG are usually being produced by a pulsating vessel, which we did not see in our data. However, it cannot be ruled out that even pulse wave artifacts, which are invisible in the ongoing EEG, become evident in an analysis exactly time locked to the R peak. The arterial pressure wave usually peaks at about 200 ms after the QRS complex and is most prominent over frontal and temporal regions. Although the wave investigated in this study peaked at around 300–400 ms after R peak, we cannot fully exclude pulse wave influences. Speaking against the positivity being a mere mechanical artifact was the fact that it was largely decreased during S2 spindles.

In a more general sense, the coupling between cardiac and encephalic activity can also be framed, such that the brain can be seen as a resonating body that responds to various forms of stimulations. The brain is never quiet, but every input always meets ongoing processes with often oscillatory characteristics. This means that input is modulating ongoing brain activity with the extent of this modulation depending on, for example, input strength or attentional amplification. This also implies that the processing of input does certainly not need to result in some form of conscious impression. The brain's property to resonate or become entrained to rhythmic external input has previously been shown by studies using photic (Becker, Gramann, Müller, & Elliott, 2009) or magnetic stimulation (Thut et al., 2011). Repetitive stimulation with a certain frequency can thereby result in so-called steady-state visual evoked potential (SSVEP; Burkitt, Silberstein, Cadusch, & Wood, 2000; Herrmann, 2001), which can follow even weak stimulation intensities such as the change between frames on a display with high refresh rates such as 75 Hz (Herrmann, Mecklinger, & Pfeifer, 1999; Lyskov, Ponomarev, Sandström, Hansson Mild, & Medvedev, 1998). The SSVEP possibly represents a mixture of repetitive evoked responses as well as entrained ongoing oscillations. Interestingly, it has been shown that the brain's oscillatory activity entrains more strongly to visual flicker stimulations in prominent inherent frequency ranges such as the gamma band around 40 Hz, which is discussed as being related to (visual) feature binding (Busch, Debener, Kranczioch, Engel, & Herrmann, 2004; Engel & Singer, 2001; Tallon-Baudry, 2009; Tallon-Baudry & Bertrand, 1999) or the alpha band (8–12 Hz) as the EEG's dominant frequency range most likely reflecting inhibitory mechanisms related to general (visual) attention, working memory processes, and semantic processing (Jensen, Gelfand, Kounios, & Lisman, 2002; Jensen & Mazaheri, 2010; Jokisch & Jensen, 2007; Klimesch, 2012; Klimesch, Fellinger, & Freunberger, 2011; Klimesch, Sauseng, & Hanslmayr, 2007; Zauner, Gruber, Himmelstoß, Lechinger, & Klimesch, 2014). In conclusion, if oscillatory brain activity can be entrained by repetitive external influences, maybe it also entrains to cardiac activity as indicated by the correlations between the HR and the EEG spectral peak frequency and the temporal coupling of heartbeats and slow oscillations.

In summary, we were able to demonstrate that during wakefulness the EEG spectral peak frequency was correlated with heart rate and that this correlation faded with increasing sleep depth. Furthermore, also frontocentral heartbeat evoked amplitude decreased with increasing levels of sleep depth, while during REM sleep evoked amplitudes were again similar to light sleep or even wake. Furthermore, amplitudes of heartbeat evoked potentials were largely decreased during sleep spindles possibly resulting from the spindle-associated thalamocortical inhibition. Spindle phase itself, however, seemed to be modulated by co-occurring R peaks. And lastly, the occurrence of heartbeats was related to the phase of high amplitude slow oscillations during deep sleep stages. The slow oscillation represents a bi-stable activation pattern of large (thalamo)cortical neuronal assemblies and has previously been shown to group the occurrence of sleep spindles.

Although we tried to give a few potential interpretations for these novel findings indicating several relationships between cardiac and cortical oscillation pattern, future research is necessary to disentangle the found relationships especially with respect to their directionality and their potential influence on cognition.

References

Achermann, P., & Borbely, A. A. (1997). Low-frequency (< 1 Hz) oscillations in the human sleep electroencephalogram. *Neuroscience*, *81*, 213–222. doi: 10.1016/S0306-4522(97)00186-3

Anderer, P., Gruber, G., Parapatics, S., Woertz, M., Miazhynskaia, T., Klösch, G., . . . Danker-Hopfe, H. (2005). An E-health solution for automatic sleep classification according to Rechtschaffen and Kales: Validation study of the Somnolyzer 24 × 7 utilizing the Siesta database. *Neuropsychobiology*, *51*, 115–133. doi: 10.1159/000085205

Bastien, C. H., Crowley, K. E., & Colrain, I. M. (2002). Evoked potential components unique to non-REM sleep: Relationship to evoked K-complexes and vertex sharp waves. *International Journal of Psychophysiology*, *46*, 257–274. doi: 10.1016/S0167-8760(02)00117-4

Becker, C., Gramann, K., Müller, H. J., & Elliott, M. A. (2009). Electrophysiological correlates of flicker-induced color hallucinations. *Consciousness and Cognition*, *18*, 266–276. doi: 10.1016/j.concog.2008.05.001

Benjamini, Y., & Hochberg, Y. (2000). On the adaptive control of the false discovery rate in multiple testing with independent statistics. *Journal of Educational and Behavioral Statistics*, *25*, 60–83. doi: 10.2307/1165312

Blanke, O. (2012). Multisensory brain mechanisms of bodily self-consciousness. *Nature Reviews Neuroscience*, *13*, 556–571. doi: 10.1038/nrn3292

Burkitt, G. R, Silberstein, R. B., Cadusch, P. J., & Wood, A. W. (2000). Steady-state visual evoked potentials and travelling waves. *Clinical Neurophysiology*, *111*, 246–258. doi: 10.1016/S1388-2457(99)00194-7

Busch, N. A., Debener, S., Kranczioch, C., Engel, A. K., & Herrmann, C. S. (2004). Size matters: Effects of stimulus size, duration and eccentricity on the visual gamma-band response. *Clinical Neurophysiology*, *115*, 1810–1820. doi: 10.1016/j.clinph.2004.03.015

Censi, F., Calcagnini, G., & Cerutti, S. (2002). Coupling patterns between spontaneous rhythms and respiration in cardiovascular variability signals. *Computer Methods and Programs in Biomedicine*, *68*, 37–47. doi: 10.1016/S0169-2607(01)00158-4

Critchley, H. D., & Harrison, N. A. (2013). Visceral influences on brain and behavior. *Neuron*, *77*, 624–638. doi: 10.1016/j.neuron.2013.02.008

Csercsa, R., Dombovári, B., Fabó, D., Wittner, L., Erőss, L. Entz, L., … Kelemen, A. (2010). Laminar analysis of slow wave activity in humans. *Brain*, *133*, 2814–2829. doi: 10.1093/brain/awq169

Cysarz, D., von Bonin, D., Lackner, H., Heusser, P., Moser, M., & Bettermann, H. (2004). Oscillations of heart rate and respiration synchronize during poetry recitation. *American Journal of Physiology–Heart and Circulatory Physiology*, *287*, H579–H587. doi: 10.1152/ajpheart.01131.2003

Dirlich, G., Vogl, L., Plaschke, M., & Strian, F. (1997). Cardiac field effects on the EEG. *Electroencephalography and Clinical Neurophysiology*, *102*, 307–315. doi: 10.1016/S0013-4694(96)96506-2

Engel, A. K., & Singer, W. (2001). Temporal binding and the neural correlates of sensory awareness. *Trends in Cognitive Sciences*, *5*, 16–25. doi: 10.1016/S1364-6613(00)01568-0

Fowles, D. C., Fisher, A. E., & Tranel, D. T. (1982). The heart beats to reward: The effect of monetary incentive on heart rate. *Psychophysiology*, *19*, 506–513. doi: 10.1111/j.1469-8986.1982.tb02577.x

Fukushima, H., Terasawa, Y., & Umeda, S. (2011). Association between interoception and empathy: Evidence from heartbeat-evoked brain potential. *International Journal of Psychophysiology*, *79*, 259–265. doi: 10.1016/j.ijpsycho.2010.10.015

Gray, M. A., Taggart, P., Sutton, P. M., Groves, D., Holdright, D. R., Bradbury, D., … Critchley, H. D. (2007). A cortical potential reflecting cardiac function. *Proceedings of the National Academy of Sciences*, *104*, 6818–6823. doi: 10.1073/pnas.0609509104

Herrmann, C. S. (2001). Human EEG responses to 1–100 Hz flicker: Resonance phenomena in visual cortex and their potential correlation to cognitive phenomena. *Experimental Brain Research*, *137*, 346–353. doi: 10.1007/s002210100682

Herrmann, C. S., Mecklinger, A., & Pfeifer, E. (1999). Gamma responses and ERPs in a visual classification task. *Clinical Neurophysiology*, *110*, 636–642. doi: 10.1016/S1388-2457(99)00002-4

Jänig, W. (1996). Neurobiology of visceral afferent neurons: Neuroanatomy, functions, organ regulations and sensations. *Biological Psychology*, *42*, 29–51. doi: 10.1016/0301-0511(95)05145-7

Jensen, O., & Colgin, L. L. (2007). Cross-frequency coupling between neuronal oscillations. *Trends in Cognitive Sciences*, *11*, 267–269. doi: 10.1016/j.tics.2007.05.003

Jensen, O., Gelfand, J., Kounios, J., & Lisman, J. E. (2002). Oscillations in the alpha band (9–12 Hz) increase with memory load during retention in a short-term memory task. *Cerebral Cortex*, *12*, 877–882. doi: 10.1093/cercor/12.8.877

Jensen, O., & Mazaheri, A. (2010). Shaping functional architecture by oscillatory alpha activity: Gating by inhibition. *Frontiers in Human Neuroscience*, *4*. doi: 10.3389/fnhum.2010.00186

Jokisch, D., & Jensen, O. (2007). Modulation of gamma and alpha activity during a working memory task engaging the dorsal or ventral stream. *Journal of Neuroscience*, *27*, 3244–3251. doi: 10.1523/JNEUROSCI.5399-06.2007

Klimesch, W. (2012). Alpha-band oscillations, attention, and controlled access to stored information. *Trends in Cognitive Sciences*, *16*, 606–617. doi: 10.1016/j.tics.2012.10.007

Klimesch, W. (2013). An algorithm for the EEG frequency architecture of consciousness and brain body coupling. *Frontiers in Human Neuroscience*, *7*. doi: 10.3389/fnhum.2013.00766

Klimesch, W., Fellinger, R., & Freunberger, R. (2011). Alpha oscillations and early stages of visual encoding. *Frontiers in Psychology*, *2*, 118. doi: 10.3389/fpsyg.2011.00118

Klimesch, W., Sauseng, P., & Hanslmayr, S. (2007). EEG alpha oscillations: The inhibition-timing hypothesis. *Brain Research Reviews*, *53*, 63–88. doi: 10.1016/j.brainresrev.2006.06.003

Lachaux, J. P., Rodriguez, E., Martinerie, J., & Varela, F. J. (1999). Measuring phase synchrony in brain signals. *Human Brain Mapping*, *8*, 194–208. doi: 10.1002/(SICI)1097-0193(1999)8:4%3C194::AID-HBM4%3E3.0.CO;2-C

Lakatos, P., Shah, A. S., Knuth, K. H., Ulbert, I., Karmos, G., & Schroeder, C. E. (2005). An oscillatory hierarchy controlling neuronal excitability and stimulus processing in the auditory cortex. *Journal of Neurophysiology*, *94*, 1904–1911. doi: 10.1152/jn.00263.2005

Lawrence, C. A, & Barry, R. J. (2010). Cognitive processing effects on auditory event-related potentials and the evoked cardiac response. *International Journal of Psychophysiology*, *78*, 100–106. doi: 10.1016/j.ijpsycho.2010.06.027

Lyskov, E., Ponomarev, V., Sandström, M., Hansson Mild, K., & Medvedev, S. (1998). Steady-state visual evoked potentials to computer monitor flicker. *International Journal of Psychophysiology*, *28*, 285–290. doi: 10.1016/S0167-8760(97)00074-3

Massimini, M., Boly, M., Casali, A., Rosanova, M., & Tononi, G. (2009). A perturbational approach for evaluating the brain's capacity for consciousness. *Progress in Brain Research*, *177*, 201–214. doi: 10.1016/S0079-6123(09)17714-2

Massimini, M., Ferrarelli, F., Esser, S. K., Riedner, B. A., Huber, R., Murphy, M., … Tononi, G. (2007). Triggering sleep slow waves by transcranial magnetic stimulation. *Proceedings of the National Academy of Sciences of the United States of America*, *104*, 8496–8501. doi: 10.1073/pnas.0702495104

Massimini, M., Ferrarelli, F., Murphy, M. J., Huber, R., Riedner, B. A., Casarotto, S., & Tononi, G. (2010). Cortical reactivity and effective connectivity during REM sleep in humans. *Cognitive Neuroscience*, *1*, 176–183. doi: 10.1080/17588921003731578

Massimini, M., Huber, R., Ferrarelli, F., Hill, S., & Tononi, G. (2004). The sleep slow oscillation as a traveling wave. *Journal of Neuroscience*, *24*, 6862–6870. doi: 10.1523/JNEUROSCI.1318-04.2004

Mies, G. W., van der Veen, F. M., Tulen, J. H. M., Hengeveld, M. W., & van der Molen, M. W. (2011). Cardiac and electrophysiological responses to valid and invalid feedback in a time-estimation task. *Journal of Psychophysiology*, *25*, 131–142. doi: 10.1027/0269-8803/a000049

Mölle, M., Eschenko, O., Gais, S., Sara, S. J., & Born, J. (2009). The influence of learning on sleep slow oscillations and associated spindles and ripples in humans and rats. *European Journal of Neuroscience*, *29*, 1071–1081. doi: 10.1111/j.1460-9568.2009.06654.x

Mölle, M., Marshall, L., Gais, S., & Born, J. (2002). Grouping of spindle activity during slow oscillations in human non-rapid eye movement sleep. *Journal of Neuroscience*, *22*, 10941–10947.

Montoya, P., Schandry, R., & Müller, A. (1993). Heartbeat evoked potentials (HEP): Topography and influence of cardiac awareness and focus of attention. *Electroencephalography and Clinical Neurophysiology*, *88*, 163–172. doi: 10.1016/0168-5597(93)90001-6

Novak, V., Novak, P., De Champlain, J., Le Blanc, A. R., Martin, R., & Nadeau, R. (1993). Influence of respiration on heart rate and blood pressure fluctuations. *Journal of Applied Physiology*, *74*, 617–617.

Palva, J. M., Palva, S., & Kaila, K. (2005). Phase synchrony among neuronal oscillations in the human cortex. *Journal of Neuroscience*, *25*, 3962–3972. doi: 10.1523/JNEUROSCI.4250-04.2005

Panitz, C., Wacker, J., Stemmler, G., & Mueller, E. M. (2013). Brain-heart coupling at the P300 latency is linked to anterior cingulate cortex and insula—A cardio-electroencephalographic covariance tracing study. *Biological Psychology*, *94*, 185–191. doi: 10.1016/j.biopsycho.2013.05.017

Park, H.-D., Correia, S., Ducorps, A., & Tallon-Baudry, C. (2014). Spontaneous fluctuations in neural responses to heartbeats predict visual detection. *Nature Neuroscience*, *17*, 612–618. doi: 10.1038/nn.3671

Park, H.-D., & Tallon-Baudry, C. (2014). The neural subjective frame: From bodily signals to perceptual consciousness. *Philosophical Transactions of the Royal Society B: Biological Sciences*, *369*, 20130208. doi: 10.1098/rstb.2013.0208

Pollatos, O., & Schandry, R. (2004). Accuracy of heartbeat perception is reflected in the amplitude of the heartbeat-evoked brain potential. *Psychophysiology*, *41*, 476–482. doi: 10.1111/1469-8986.2004.00170.x

Rechtschaffen, A., & Kales, A. A. (1968). *A manual of standardized terminology, techniques and scoring system for sleep stages of human sujects*. Bethesda, MD: U. S. Department of Health, Education, and Welfare Public Health Service–NIH/NIND.

Saul, J. P., Kaplan, D. T., & Kitney, R. I. (1988). Nonlinear interactions between respiration and heart rate: Classical physiology or entrained nonlinear oscillators. *Computers in Cardiology*, *1988*, 299–302. doi: 10.1109/CIC.1988.72621

Schabus, M., Dang-Vu, T. T., Albouy, G., Balteau, E., Boly, M., Carrier, J., … Maquet, P. (2007). Hemodynamic cerebral correlates of sleep spindles during human non-rapid eye movement sleep. *Proceedings of the National Academy of Sciences of the United States of America*, *104*, 13164–13169. doi: 10.1073/pnas.0703084104

Schabus, M., Gruber, G., Parapatics, S., Sauter, C., Klosch, G., Anderer, P., … Zeitlhofer, J. (2004). Sleep spindles and their significance for declarative memory consolidation. *SLEEP*, *27*, 1479–1485.

Schandry, R., & Weitkunat, R. (1990). Enhancement of heartbeat-related brain potentials through cardiac awareness training. *International Journal of Neuroscience*, *53*, 243–253. doi: 10.3109/00207459008986611

Schimicek, P., Zeitlhofer, J., Anderer, P., & Saletu, B. (1994). Automatic sleep-spindle detection procedure—Aspects of reliability and validity. *Clinical EEG and Neuroscience*, *25*, 26–29. doi: 10.1177/155005949402500108

Steriade, M., Contreras, D., Curro Dossi, R., & Nunez, A. (1993). The slow (<1 Hz) oscillation in reticular thalamic and thalamocortical neurons: Scenario of sleep rhythm generation in interacting thalamic and cortical networks. *Journal of Neuroscience*, *13*, 3284–3299.

Steriade, M., McCormick, D. A., & Sejnowski, T. J. (1993). Thalamocortical oscillations in the sleeping and aroused brain. *Science*, *262*, 679–685. doi: 10.1126/science.8235588

Tallon-Baudry, C. (2009). The roles of gamma-band oscillatory synchrony in human visual cognition. *Frontiers in Bioscience*, *14*, 321–332. doi: 10.2741/3246

Tallon-Baudry, C., & Bertrand, O. (1999). Oscillatory gamma activity in humans and its role in object representation. *Trends in Cognitive Science*, *3*, 151–162. doi: 10.1016/S1364-6613(99)01299-1

Thayer, J. F., & Lane, R. D. (2009). Claude Bernard and the heart–brain connection: Further elaboration of a model of neurovisceral integration. *Neuroscience & Biobehavioral Reviews*, *33*, 81–88. doi: 10.1016/j.neubiorev.2008.08.004

Thut, G., Veniero, D., Romei, V., Miniussi, C., Schyns, P., & Gross, J (2011). Rhythmic TMS causes local entrainment of natural oscillatory signatures. *Current Biology*, *21*, 1176–1185. doi: 10.1016/j.cub.2011.05.049

van der Veen, F. M., van der Molen, M. W., Crone, E. A., & Jennings, J. R. (2004). Phasic heart rate responses to performance feedback in a time production task: Effects of information versus valence. *Biological Psychology*, *65*, 147–161. doi: 10.1016/j.biopsycho.2003.07.003

Zauner, A., Gruber, W., Himmelstoß, N. A., Lechinger, J., & Klimesch, W. (2014). Lexical access and evoked traveling alpha waves. *NeuroImage*, *91*, 252–261. doi: 10.1016/j.neuroimage.2014.01.041

(Received January 13, 2015; Accepted July 19, 2015)